Chapter 6

Inversion of potential field data by Genetic Algorithms

In this chapter the application of Genetic Algorithms to the inversion of potential field data is discussed. I present a Genetic Algorithm that simultaneously generates a large number of different solutions to various potential field inverse problems. It is shown that in simple cases a satisfactory description of the ambiguity domain inherent in potential field problems can be efficiently obtained by a simple analysis of the ensemble of solutions. From this analysis information about the expected bounds on the unknown parameters as well as a measure of the reliability of the final solution can also be obtained, that can not be recovered with local optimisation methods. I discuss how the algorithm can be modified to address large dimensional problems. This can be achieved by the use of the pseudo subspace method, already presented in Chapter 4, as well as by subdividing the overall calculation domain into a number of small subdomains. The effectiveness and flexibility of the method is shown on a range of different potential field inverse problems, both in 2-D and 3-D, on synthetic and field data. The material presented in this chapter has been submitted to GEOPHYSICAL PROSPECTING and it is currently under final review.

6.1 Introduction

Different techniques are available in exploration geophysics in order to obtain information on the distribution of minerals in the subsurface. Among these, the analysis of potential field data is of great interest because it is far less expensive than most of other investigation methods.

Similarly to other geophysical applications, the analysis of potential field data is usually formulated as an inverse problem, in which a set(s) of geological parameters is sought that define mathematical models which reproduce the observed data in a satisfactory fashion.

As for the seismic refraction problem presented in Chapter 5, traditionally potential field data inverse problems have been approached by the use of local optimisation techniques. However, two main problems may limit the effectiveness of this approach. First, when the shape of the geological bodies responsible for the potential field anomaly is sought together with their density and/or magnetic properties, the mathematical formulation of the inverse problem becomes highly non-linear [1]. As extensively discussed in the previous chapters, on highly non-linear problems local searches are prone to trapping in local minima. In these circumstances an appropriate choice of a starting model is necessary in order to obtain satisfactory results. Also, information about the curvature in the solution space are needed by these algorithms to search the solution domain.

Secondly, ambiguity is inherent in the inversion of potential field data, i.e. a large number of solutions can be found that satisfy the constrains of the problem equally well [2]. Again inversion methods that search the solution space for a single minimum are not suitable for these problems because a single solution can hardly be representative of the ambiguity domain. Traditionally this problem has been tackled by limiting the ambiguity through the use of appropriate constraints. However, this requires detailed 'a priori' information on the nature of these constraints, that often is not available on geophysical problems. Recently, a new approach to ambiguity problem has been proposed [11, 3] in which a large number of solutions that fit the data is collected. Different statistical tools may then be used to analyse the ensemble of the solutions and to describe the shape of

the ambiguity domain.

One of the main features of Genetic Algorithms is that they work by modifying a population of solutions, rather that a single solution, as most traditional algorithms. Consequently, they are able to explore different areas of the search space at the same time. This not only sensibly reduces the risk of getting trapped in local minima very far from the global one, but also allows for the simultaneous optimisation of a large number of solutions which may help to address ambiguity problems.

These factors, together with the promising results obtained in the seismic refraction problem, suggest that genetic Algorithms could be successfully applied to other areas of geophysics, including potential field inverse problems. This application is described in this chapter.

The Genetic Algorithm here presented does not include any problem specific operator. Accordingly, the algorithm can be applied equally well to the inversion of gravity and magnetic data, either separately or simultaneously. The method potential has been tested on three different applications. In the first test a gravity and a magnetic synthetic data set have been simultaneously inverted. In the description of this experiment details on how the simultaneous inversion has been performed, as well as outlines on the statistical analysis of the ensemble of solutions obtained by the Genetic Algorithm are given. In the second test a real gravity data set has been inverted in order to reconstruct the shape of a sedimentary basin in Western Australia. A slightly different implementation of the algorithm is described that allows for the inversion of very long profiles with a computational effort proportional to the profile length. In the last experiment I show that the method can be easily extended to some 3-D problems. This is described in the inversion of a real magnetic data set from the Auckland volcanic field, New Zealand.

6.2 Genetic Algorithms implementation

The main aim in this experiment is to collect a large number of different acceptable solutions in order to attempt a statistical description of the ambiguity inherent in

the inversion of potential field data. These solutions must be as different as possible one from each other to enable their statistical analysis to be representative of the ambiguity domain. In order to obtain differing solutions diversity must be kept in the Genetic Algorithm population. The GA operator mostly responsible for manteining diversity inside the population is selection. In Chapter 4 I showed how parent selection allows for larger diversity to be manteined compared to linear normalisation selection. Accordingly, a Genetic Algorithm incorporating parent selection has been employed in this analysis. The reader is refered to Chapter 4 for more details about the selection operators and the Genetic Algorithms implementations.

6.3 2-D simultaneous inversion of magnetic and gravity data

Recently a number of authors have proposed to simultaneously invert gravity and magnetic data in order to reconstruct the shape of buried geological bodies [12, 7]. The rationale behind this procedure is that the ambiguity inherent in the inversion of potential field data is highly reduced when the two data sets are combined.

In the 2-D inversion of magnetic and gravity data I aim at reconstructing the lower contact between two geological bodies of different density and magnetic susceptibility as well as the value of the density and magnetic susceptibility contrast. In my applications this is achieved by reconstructing the depth of the contact at regularly spaced nodes whose horizontal position is kept fixed.

In the example presented in this section the anomalous body is constrained to outcrop between the extreme nodes. This configuration has been adopted to simplify the problem geometry, but similar inversion processes could also be implemented without this constraint.

In Chapter 4 I introduced the 'pseudo subspace' and its effect in the Genetic Algorithm process. Figure 4.7 shows how the method is implemented in this application. Note that the lateral boundaries are determined by 4 nodes that are fixed both horizontally and vertically throughout the inversion. The method is implemented in three stages. In the first stage of the Genetic Algorithm search,

the body is described by the 4 fixed nodes plus 5 nodes whose vertical position is allowed to vary (black dots in Figure 4.7a). In subsequent generations the spacing of the nodes is halved. New nodes are inserted and they are given a depth value equal to the average depth of the adjacent nodes. This guarantees that the best solutions found so far are passed unaltered to the next stage. Now the body is described by 9 nodes with variable depth plus the 4 fixed ones (see Figure 4.7b). This process is repeated one more time with a grid of 17 nodes (Figure 4.7c), whereupon the Genetic Algorithm is run until an acceptable convergence is reached.

I applied the Genetic Algorithm to the inversion of gravity and magnetic data for the example described in Figure 6.1. The boundaries of a synthetic body are represented by the thick line in Figure 6.1c. The density contrast of the synthetic body relative to the surrounding geology is $-0.15\ t/m^3$ while the susceptibility contrast is assumed to be $0.4\ 10^3\ S.I.$. Figure 6.1a and 6.1b show the gravity and magnetic anomalies. The two synthetic anomalies have been simultaneously inverted in order to reconstruct the shape of the synthetic body.

Different procedures may be employed when information from different data sets are combined in the same inversion process. Lines [6] offers a good overview of some of these choices. One possibility is to sequentially invert the different data sets and use the output from one inversion as the starting model for the inversion of the next data set. This procedure is well suited to local optimisation techniques, in which a starting model is needed. It has the advantage of not requiring any weighting between the different data sets, but it has the disadvantage that it gives less control on the actual fit of both the data sets. A further discussion of the advantages and disadvantages of this procedure can be found in [6].

I chose to invert the data sets simultaneously with the objective function to be optimised represented by a combination of the individual misfits. In this way the information from the multiple data sets are simultaneously used. This choice is better suited for global optimisation and also it gives a better control on the misfit of both the data sets. In my experiment I used the following misfit expression:

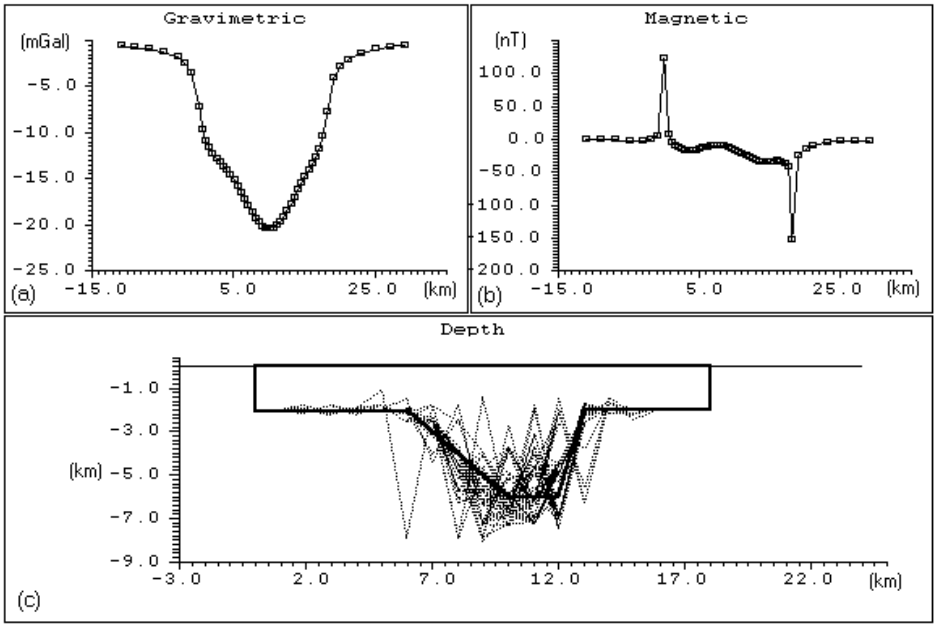

Figure 6.1: Simultaneous inversion of magnetic and gravity synthetic data. The synthetic gravity and magnetic anomalies (thick lines) together with the computed anomalies for the best solution from the inversion (scattered points) are shown in Figure 6.1a and 6.1b, respectively. In Figure 6.1c the synthetic body used to generate such anomalies (thick line) is shown together with the best 60 solutions from the Genetic Algorithm inversion (dashed lines). As we can see the ambiguity inherent in this problem allows for very different solutions to satisfy the data equally well.

$$Misfit = W_{mag}\frac{\sum_1^{mstat}|\frac{M_{obs}-M_{synth}}{M_{synth}}|^2}{mstat} + W_{grav}\frac{\sum_1^{gstat}|\frac{G_{obs}-G_{synth}}{G_{synth}}|^2}{gstat} \qquad (6.1)$$

where M is the magnetic measurement, G the gravity one, $mstat$ the number of stations for magnetic measurement, $gstat$ the number of stations in the gravity model, and W_{mag} and W_{grav} are the weights given to the magnetic and gravity misfit, respectively. The choice of the weights is usually problem specific. In some cases the choice may depend on the different accuracy of the particular data sets, in other cases it may depend on the different degree of ambiguity inherent in a data set. In my case, since I deal with two noise free data sets, each with a large degree of ambiguity and normalised squared errors I chose to give the same weight

to the gravity and magnetic misfits, i.e., $W_{mag} = W_{grav}$.

In the Genetic Algorithm inversion, the last stage involving the pseudo subspace method was reached after 60 generations. Now with a population of 100 individuals the Genetic Algorithm was allowed to run for another 100 generations. The result of the inversion can be seen in Figure 6.1. Figure 6.1c shows the best 60 solutions superimposed one to the other. For each of these solutions the error misfit is approximately zero. The calculated anomaly for the 60 solutions is shown in Figure 6.1a and 3b as scattered points. As can be seen the agreement with the synthetic data (thick line) is good. This result is achieved because of the ability of the procedure to find an approximately correct value for the density and susceptibility contrasts in the early stages of the inversion. The density contrast obtained was $-0.16\ t/m^3$ ($-0.15\ t/m^3$ assumed for the synthetic model) and the magnetic susceptibility contrast as $0.38\ 10^3\ S.I.$ (versus $0.4\ 10^3\ S.I.$ for the synthetic value) and only very limited variations could be found among the different solutions. The reason for this is that the anomalous body is constrained to outcrop between the lateral points, that largely reduce the ambiguity in the problem. Further comments on the influence of this configuration is given in the 'Discussion' at the end of the chapter. This accurate information is then exploited in the successive higher dimensional stages to better define the shape of the body. However, the shape of the solutions differ widely and this gives a measure of the degree of the ambiguity still inherent in this problem.

A better description of this observed ambiguity is achieved by calculating the arithmetic average and the variance of the solutions for each parameter. This is shown in Figure 6.2. Figure 6.2c shows the synthetic model (thick line), the average of the solutions (dashed line) and the variance of each node depth (vertical bars). As can be seen the average solution is a smooth but reasonably good approximation of the assumed synthetic model. The variance bars give an indication of the reliability of assuming the average to be the result of the inversion. The larger the bar corresponding to one node the less reliable the depth. Also, this analysis gives an estimate of the bounds on the values the parameters can assume in the inversion.

This information could not be obtained with traditional methods unless spe-

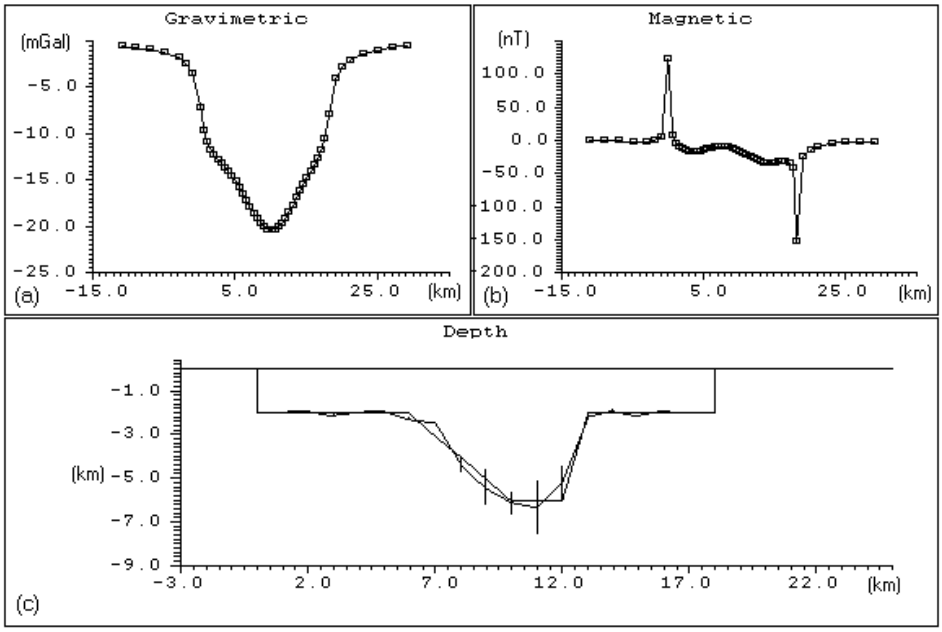

Figure 6.2: Statistical analysis of the best 60 solutions from the Genetic Algorithm inversion. The arithmetic average (dash line) and the variance of the solutions for each parameter (vertical lines) are shown in Figure 6.2c together with the synthetic model (thick line). In Figure 6.2a and 6.2b the synthetic (thick line) and the computed anomalies for the average solution are shown.

cific 'a priori' information about the parameters distribution was included in the inversion. As it has been shown, a Genetic Algorithm does not require this kind of 'a priori' information and the description of the ambiguity domain is simply the result of its ability to sample different areas of the solution space at the same time and to reconstruct a large number of different solutions.

Al-Chalabi [1] and Vasco et alii [11] tried to give a geometrical description of the ambiguity inherent in magnetic and gravity problems using very different analysis techniques. According to their work, this ambiguity belongs to a non-normal, quadratic distribution. I performed a similar analysis for my problem and their result was confirmed. Accordingly, more sophisticated statistical tools than a simple arithmetic average should be used to describe these distributions. Nevertheless, the results presented in this section suggest that for practical applications the simple statistics I adopted may give satisfactory results. The demonstration can be found in Figure 6.2a and Figure 6.2b. The gravity and magnetic anomalies

due to the average solution in Figure 6.2c are presented as scattered points. As it can be seen, the agreement with the synthetic anomalies is good. Also, these pictures are almost indistinguishable from the ones in Figure 6.1a and 6.1b where the agreement between the calculated anomalies for the 60 solutions found by the Genetic Algorithm and the synthetic anomalies is presented. This shows that the arithmetic average of the best solutions reproduces the synthetic data in a satisfactory fashion despite it does not belong to the solutions quadratic distribution (because of its non-normality).

In geological/geophysical analysis it is often desirable to reduce the ambiguity inherent in the data sets as much as possible. Usually this is achieved by introducing a priori constrains in the problem. Where detailed 'a priori' information is present this can be easily included in the Genetic Algorithm process, for example by fixing some of the unknown parameters. However, obtaining information about the extent of the ambiguity gives in turn indications on how and where to direct further surveying in order to further reduce the ambiguity. If a more reliable description of the geology under analysis is required, it would be appropriate to perform further geological/geophysical surveying at the locations where the variance is larger. The correct assessment of the poorly determined nodes would consequently also strongly reduce the ambiguity in the rest of the domain.

6.4 2-D inversion of real gravity data

I now present the inversion of a 120 km long real data set from a gravity survey across Perth basin, in Western Australia. The aim of the inversion process is to detect the shape of a deep graben consisting of Permian to Holocene sedimentary rocks, with average density contrast with the background is $-0.4\ t/m^3$, bounded by the Darling Fault to the east and by the Busselton Fault to the west.

Very large dimensional problems usually arise in inverting long profiles. When an inverse problem has high dimensionality the efficiency of a Genetic Algorithm, as for any inversion procedure, may be reduced by the following factors: (i) increase in the computation cost for function evaluations, (ii) increase in ambiguity problems and (iii) a corresponding increase in the volume of the search domain.

The last point is particularly important because, for computational reasons, the increase can not be compensated for by a similar increase in the size of the Genetic Algorithm population. Consequently, attention should be paid to keeping the problem dimensionality as low as possible.

Thus, it is useful to modify the implementation of the Genetic Algorithm as described above in order to simplify the inversion of long gravity profiles. The modification consists in reconstructing the graben section by section and it is described with the help of Figure 6.3. In Figure 6.3a the reconstruction of the part of the profile between 35 and 65 kilometres only is attempted. This is achieved by concentrating the depth nodes within this section in order to obtain a satisfactory fit between calculated and observed data in this part of the profile. The regions corresponding to the lateral sections of the domain, (i.e. between 0 and 35 kilometres and between 65 and 130 kilometres in Figure 6.3a) are modelled by the use of two rectangles whose depths are varied to compensate for the corresponding parts of the gravity profile. In the top part of the Figure 6.3a the observed gravity anomaly is presented as a thin line, while the calculated one is represented by the thick line. As it can be seen the lines agree in the section under analysis, while the thick line gives just a rough average of the anomaly on the remaining of the profile. Once the agreement between the measured and the calculated data on the section under analysis has been achieved, the procedure may be repeated on a adjacent area by progressively shifting the calculation domain horizontally along the overall profile. This is shown in Figure 6.3b and 6.3c where the reconstruction of the central part and of the eastern part of the graben, respectively, is performed.

When this moving technique is adopted the dimensionality of the inversion depends only on the number of depth nodes inside the moving section. Thus, the inversion of long profiles is reduced to several small-dimensional inverse problems, whose required computation time is equal. This means that the computation time required for the inversion of the overall profile is simply proportional to the number of sections the profile is divided into, i.e., to the profile length. The length of the profile does not affect the dimensionality, and accordingly the complexity, of the problem and consequently this technique can deal with long profiles, regardless of length. A similar approach has been used in the inversion of seismic refraction

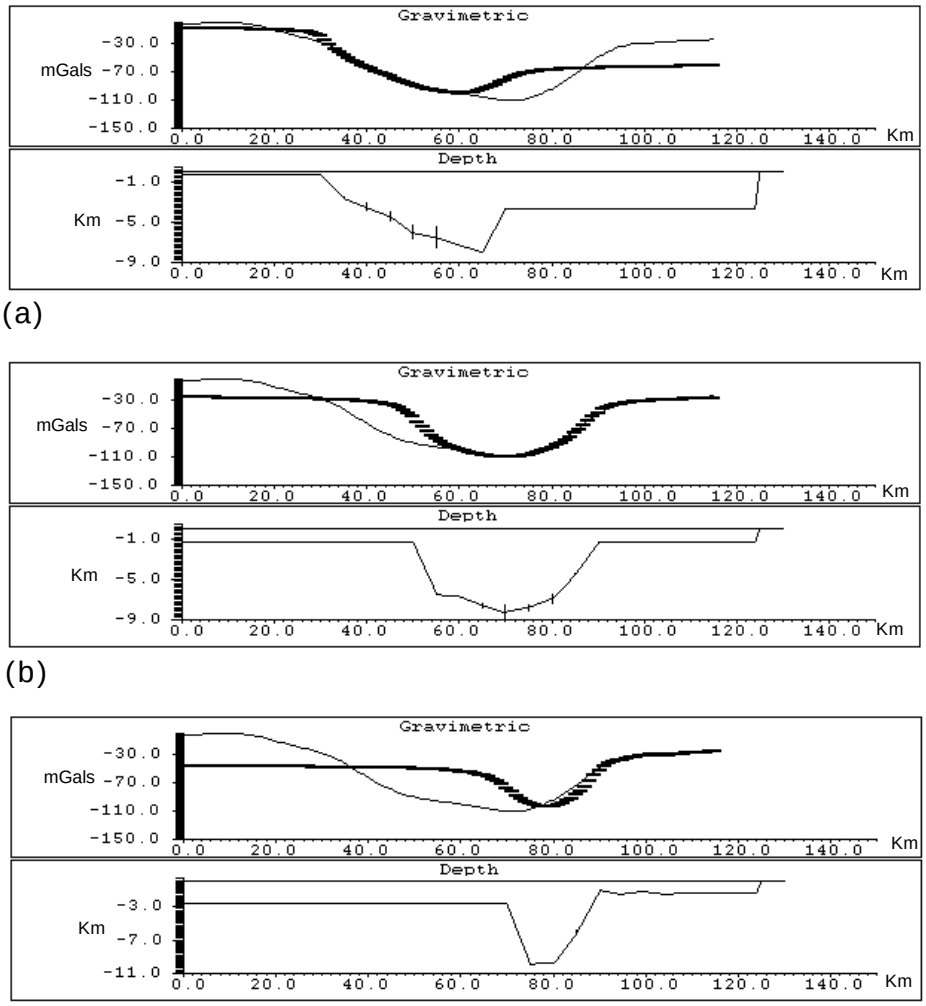

Figure 6.3: Staged inversion of long gravity profiles. In the first stage (a) only the reconstruction of the Busselton fault to the West is attempted. The body described in the bottom part of the picture reconstructs the anomaly in the corresponding part of the profile. The rectangles at the two sides are meant to give an average compensation of the lateral parts of the profile. In Figure (b) and (c) the same process is applied to the central part of the graben and to the Darling fault to the East, respectively.

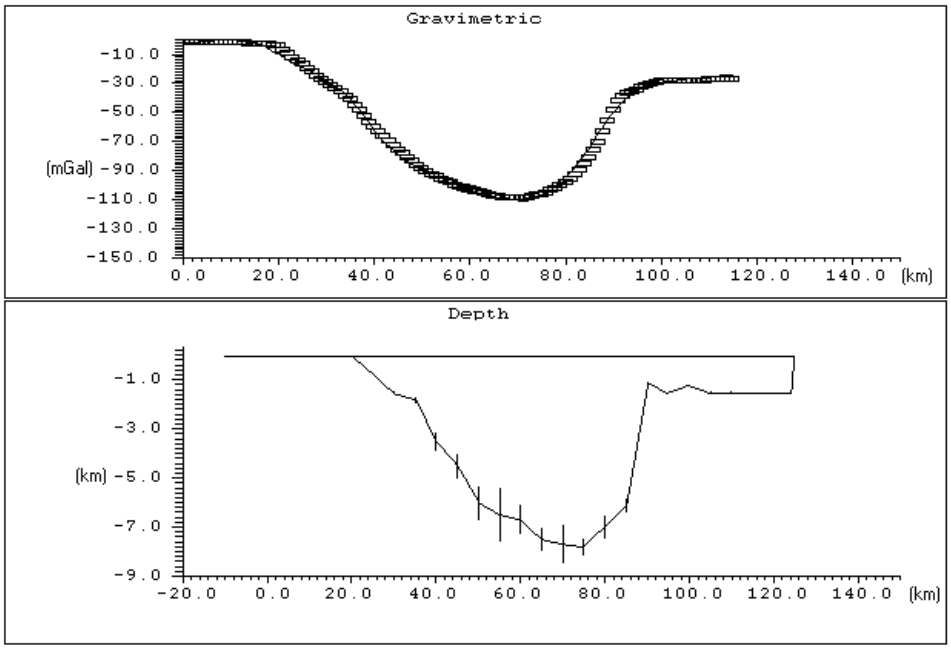

Figure 6.4: Final result from the inversion of the gravity profile on Perth basin. The good agreement between measured and observed data is shown in Figure 6.4a, while the reconstruction of the graben in presented in Figure 6.4b. The result agrees well with previous analysis of the same area shown in Figure 6.5.

data in Chapter 5.

However, if the moving technique was not employed, a number of equally spaced calculation points, proportional to the profile length, would be required. In this case the dimensionality and complexity of the problem would be affected by the profile length and consequently the computational cost of the inversion would become prohibitive at the increase of the profile length, because of the increase in function evaluation cost for bodies described by higher number of nodes, and larger population and longer convergence required by the Genetic Algorithms process to cope with the larger dimensional space, as previously stated at the beginning of the section.

The final result of the procedure can be seen in Figure 6.4 where the overall anomaly is presented. The result is compared with a previous analysis of a close parallel gravity profile in the same area (see Figure 6.5 from [5]) that has been reconstructed by interactive inversion starting from a solution obtained from seismic profiles. Both solutions satisfy the measured gravity data and give a similar

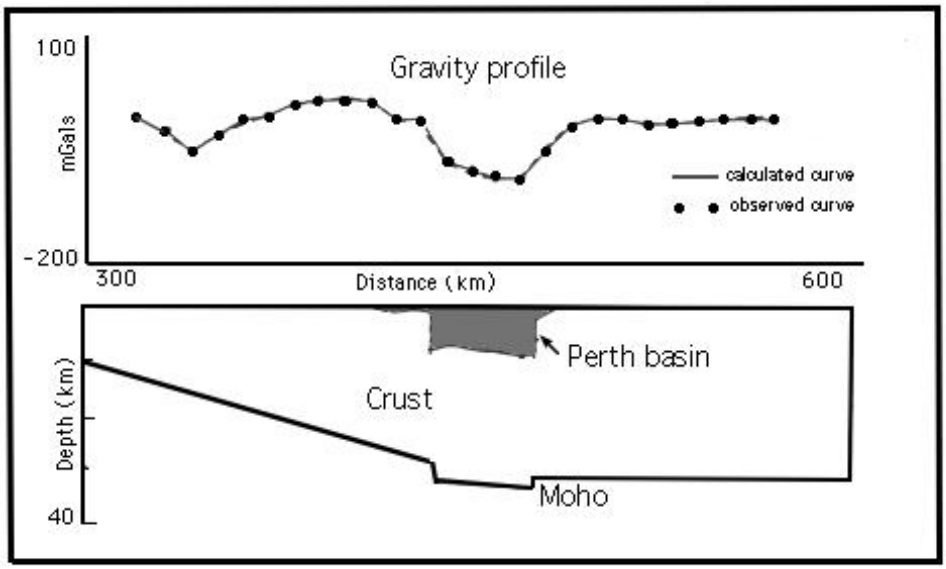

Figure 6.5: Previous study of the gravity profile on Perth basin. The image is the result of an interactive inversion of the gravity data set starting from a solution obtained by analysis of seismic data.

estimate of the depth of the sedimentary basin. However, Figure 6.4 contains additional information in the vertical bars representing the variance in the depth assessment at each node. The average solution should be considered simply the most likely or the smoothest among the family of solutions found through the use of the Genetic Algorithm. The variance bars give an additional indication on the reliability of the reconstruction. This ambiguity could not be accurately represented by a single solution as shown in Figure 6.5.

This technique exploits the close and simple spatial relationship between the geometric position of a density anomalous body and the corresponding perturbation in the gravity profile. This relationship is only slightly affected by the lateral distribution of other density anomalies. This is not true for magnetic profiles and the extension of this technique to the inversion of magnetic data is less straightforward and currently under analysis.

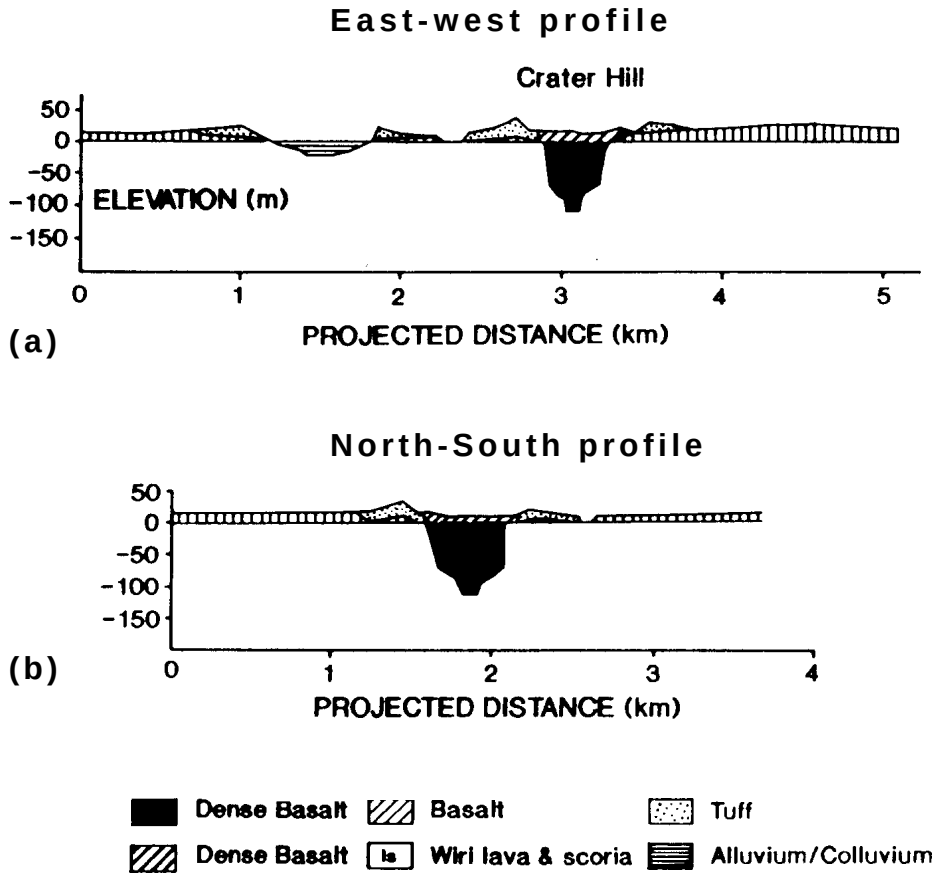

Figure 6.6: Previous geological reconstruction of the Crater Hill volcano (Papatoetoe Group). East-West profile (a) and North-South profile (b).

6.5 Extension to the 3-D case

Often magnetic/gravity data are collected over a 2-D region of the earth surface. Inverting the data to reconstruct the 3-D shape of the geological body responsible for the measured anomaly can be achieved, using Genetic Algorithms, if we replace the line of fixed points in the previous example by a 2-D regular grid of fixed points and similarly determine the depth of the contact between the body and the background geology at these points.

The method has been tested on a real magnetic data set collected in the Auckland volcanic field, New Zealand. This is the youngest of a set of mainly basaltic Pliocene to Recent intraplate volcanic associations in the New Zealand North Island. A detailed geophysical survey, correlated geological and geochemical information available on the area, had been previously performed on the area. De-

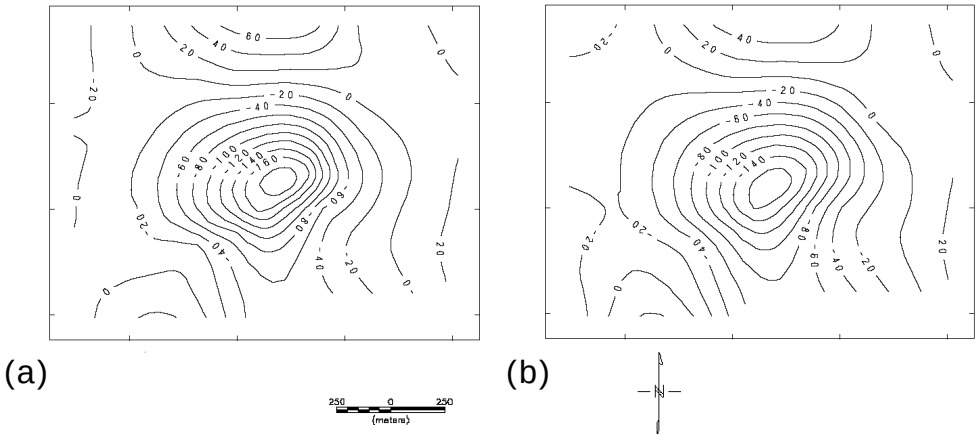

Figure 6.7: Observed magnetic field(expressed in nT) correspondent to the Crater Hill volcano area (Figure 6.7a). In (Figure 6.7b) the magnetic field correspondent to the average of the solutions found by the Genetic Algorithm is presented. As we can see the agreement is very satisfactory. Disagreements can be noticed in correspondence with the negative pick at the centre and in minor departures on the left-hand side of the picture.

tails about this survey and its results can be found in [9]. The reconstruction of one of these volcanic centres, the Crater Hill volcano (Papatoetoe Group) is shown in Figure 6.6a and 6.6b as East-West and North- South geological sections taken from [9]. In the experiment presented here the source of the observed magnetic field presented in Figure 6.7a is the volcanic plug shown in Figure 6.6.

The program GRV3TOPO [10] has been used as forward routine in the inversion process. This has been performed on a 9 x 9 regular grid with 250 m spacing both in northing and easting directions. In this case the bulk magnetisation, inclination and declination of the anomalous body has been given as 'a priori' information in the problem. The corresponding 81 dimensional space represents a relatively large dimensional problem. However, the use of the pseudo subspace method helped in tackling such high dimensionality. The Genetic Algorithm inversion has been performed again in three stages. In the first stage the body is described by a 3 x 3 grid. In the second stage the grid spacing is halved and the body in described by a 5 x 5 matrix, while in the last stage the final configuration of 9 x 9 nodes is reached. Figure 6.8 shows the 3-D representation of the average of the depth solutions from the Genetic Algorithm inversion. The North-South and East-West

profiles are shown in Figure 6.9 in order to facilitate the comparison with Figure 6.6. The corresponding calculated magnetic anomaly is shown in Figure 6.7b. The overall fit is good. Minor disagreements are present in the negative pick at the center of the magnetic contour, whose intensity in not perfectly recovered (190 nT for the observed magnetic field versus 170 nT in the calculated one) and in some lateral areas. Also, it should be noted that reconstruction in Figure 6.8 presents undulations on the lateral areas that are not present in the sections in Figure 6.6 and that the North- South profile in Figure 6.9 is larger than the one in Figure 6.6. This is probably due to the fact that only one anomalous body has been reconstructed in my experiment, and accordingly the 20-30 m tuff and basalt cover overlying the main body shown in Figure 6.6 has not been modelled.

6.6 Discussion

A number of points deserve further discussion. Traditional local optimisation methods have been applied to the inversion of real potential field data with hundreds of parameters [8]. Usually global optimisation techniques are applied to much smaller dimensional spaces, rarely exceeding a few tens of parameters [4]. This is the price paid for the advantage inherent in a global optimisation in complex problems. Often the complexity of a problem and the lack of a priori information may force the use of a global optimisation technique despite such limitations. Also, the use of the pseudo subspace method may allow the application to much larger dimensional spaces as shown in Chapter 5. Accordingly, the 81 dimensional solution space inverted in the example described in the previous section should not be considered as some maximum for Genetic Algorithm application to this kind of problem.

Furthermore, global inversion techniques are far more expensive than local methods. It has already been mentioned that an increase in computational effort may be required by the complexity of the problem, mainly due to its high non-linearity. The 2-D simultaneous inversion of magnetic and gravity data as described above required approximately 15 minutes of CPU time on a SUN SPARCSTATION 20 while approximately 50 minutes were required by the 3-D inversion.

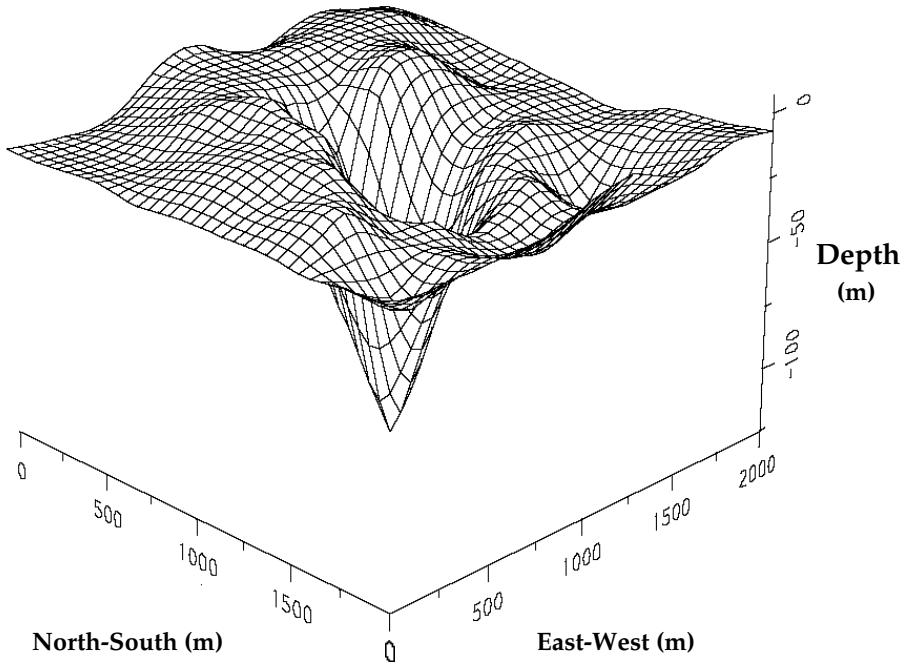

Figure 6.8: 3-D reconstruction of the anomalous body responsible for the magnetic anomaly in Figure 6.7a. The depth of the body agrees with what reconstructed in Figure 6.6. The undulation at the sides of the main body are due to thin geological layers overlaying the main body not modelled in this experiment.

This is still a reasonable result, especially when compared with the amount of time required by the collection and preprocessing of the raw data. Furthermore, with such computational effort not one but a large number of solutions have been found. A large number of solutions with local optimisation techniques could be obtained with a number of runs *at least* equivalent to the desired number of solutions, provided each run can converge towards different areas of the solution space, which is rarely guaranteed. Consequently any general assumption of high cost in the use of Genetic Algorithm should not be taken for granted, rather analysed problem by problem.

The examples presented in this chapter are characterised by relatively simple geometries, and their aim was to recover the shape and the density and/or magnetic contrast of a single anomalous body with a simple geological background. It has been shown that in these cases the simple statistics employed in this analysis was sufficient to describe the ambiguity domain in a satisfactory fashion. More

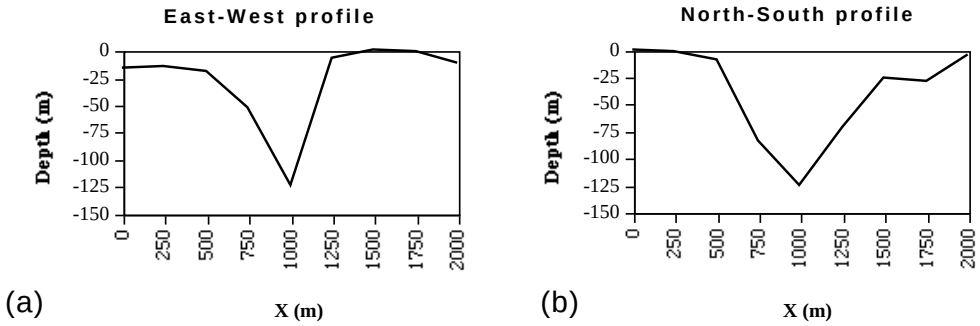

Figure 6.9: North-South (a) and East-West (b) sections of the 3-D body presented in Figure 6.7. It can be noticed that the depth and approximate shape of the main body agree with the reconstruction presented in Figure6.6.

complex geometries, i.e. in which more that one geological contact is modelled in the vertical direction, could still be modelled with this method. However, much stronger ambiguity problems should be expected. This is particular true if the body was not constrained to outcrop and the average depth of the models was allowed to vary sensibly. In such case the simple statistics used in this work is not expected to give satisfactory results and consequently more sophisticated methods should be used. A review of such tools can be found in[11].

6.7 Conclusions

As already demonstrated on other geophysical applications, Genetic Algorithms proved to be able to address the non-linearity involved in the inversion of magnetic and gravity data. Also, they showed to be an effective tool to reconstruct a number of solutions large enough to make the statistical description of the ambiguity inherent in this kind of problempossible. From this description not only a satisfactory model of the shape of the geological body under analysis may be recovered, but also useful information about the reliability of such reconstruction as well as indications on where to concentrate further geological and geophysical surveys may be obtained. Tests showed that the technique works well with synthetic as well as with real data sets both in 2-Dand 3-D. Currently the applicability of the method is limited to the reconstruction of the contact between a single anomalous body and the background, and should be regarded as a fast tool for a preliminary

analysis of magnetic and gravity data.

Bibliography

[1] M. Al-Chalabi. Interpretation of gravity anomalies by non-linear optimization. *Geophysical Prospecting*, 20:1–16, 1971.

[2] M. Al-Chalabi. Some studies relating to nonuniqueness in gravity and magnetic inverse problems. *Geophysics*, 36:835–855, 1971.

[3] S. Fraiha and J. Silva. Factor analysis of ambiguity in geophysics. *Geophysics*, 59:1083–1091, 1994.

[4] D. E. Goldberg. *Genetic algorithms in search, optimization and machine learning*. Addison-Wesley Publishing Company, Inc., 1989.

[5] R. Iasky, R. Young, and M. Middleton. Structural study of the Southern Perth Basin by geophysical methods. *Exploration Geophysics*, 22:199–206, 1991.

[6] L. R. Lines, A. K. Schultz, and S. Treitel. Cooperative inversion of geophysical data. *Geophysics*, 53:8–20, 1988.

[7] V. Menichetti and A. Guillen. Simultaneous interactive magnetic and gravity inversion. *Geophysical Prospecting*, 31:929–944, 1983.

[8] D. W. Oldenburg. The inversion and interpretation of gravity data. *Geophysics*, 39:526–536, 1974.

[9] D. J. Rout, J. Cassidy, C. A. Locke, and E. M. Smith. Geophysical evidence for temporal and structural relationships within the monogenic basalt volcanoes of the auckland volcanic field, northern new zealand. *Journal of volcanology and geothermal research*, 57:71–83, 1992.

[10] S. Soengkono. *Geophysical study of the western Taupo Volcanic zone.* PhD thesis, University of Auckland, 1990.

[11] D. W. Vasco, L. R. Johnson, and E. L. Majer. Ensemble inference in geophysical inverse problems. *Geophysical Journal International*, 115:711–728, 1993.

[12] H. Zeyen and J. Pous. 3-d joint inversion of magnetic and gravimetric data with a priori information. *Geophysical Journal International*, 112:244–256, 1993.